30TH INTERNATIONAL COSMIC RAY CONFERENCE

Energy spectrum of cosmic iron nuclei measured by H.E.S.S.

R. BÜHLER[1] FOR THE H.E.S.S. COLLABORATION
[1]*Max-Planck-Institut für Kernphysik, P.O. Box 103980, D 69029 Heidelberg, Germany*
rolf.buehler@mpi-hd.mpg.de

Abstract: A recently proposed novel technique for the detection of cosmic rays with arrays of *Imaging Atmospheric Cherenkov Telescopes* is applied to data from the High Energy Stereoscopic System (H.E.S.S.). The method relies on the ground based detection of Cherenkov light emitted from the primary particle prior to its first interaction in the atmosphere. The charge of the primary particle (Z) can be estimated from the intensity of this light, since it is proportional to Z^2. Using H.E.S.S. data, an energy spectrum for cosmic-ray iron nuclei in the energy range 13–200 TeV is derived. The reconstructed spectrum is consistent with previous direct measurements and is the most precise measurement so far in this energy range.

Introduction

At present the best measurements of elemental composition of cosmic rays in the energy range 1 GeV to 0.5 PeV come from long duration balloon flights [10]. Because of the decreasing flux of cosmic rays and the limited collection area of these experiments ($\approx$1 m^2), it is hard to extend such measurements to higher energies. A further improvement in the accuracy and energy range of composition measurements of cosmic rays could however provide crucial information about the acceleration mechanism and propagation of these particles.

In 2001, Kieda et al. [2] proposed a new method for the measurement of cosmic rays with ***I**maging **A**tmospheric **C**herenkov **T**elescopes* (IACTs). The measurement from the ground takes advantage of the huge detection area ($\approx 10^5$ m^2) of IACTs, in principle enabling the extension of spectral and composition measurements up to $\sim$ 1 PeV. Here we review this technique and describe its application to data from the *High Energy Stereoscopic System* (H.E.S.S.). We present the measurement of the iron spectrum and give an outlook on future applications of this method (a more detailed descripton of the analysis and the results can be found in [5]).

Technique

When cosmic rays enter the atmosphere they emit Cherenkov light (so called ***D**irect **C**herenkov Light*) above an element-dependent energy threshold. The Cherenkov angle increases with the density of the surrounding medium. The emission angle of the DC-light therefore increases with increasing depth of the primary particle in the atmosphere, creating a light cone on the ground with a radius of roughly 100 m (see Fig. 1). At a typical height of 30 km the particle interacts and a particle cascade is induced (Extensive Air Shower, EAS). The Cherenkov light from these secondary particles creates a second, wider, light cone on the ground.

The intensity of the DC-light is proportional to the square of the charge Z of the emitting particle, and can therefore be used to identify the primary particle. The challenge for detecting DC-light is to distinguish it from the $\approx$100 times brighter EAS-light background. Because the DC-light is emitted higher in the atmosphere, it is emitted at a smaller angle than the EAS-light, and is therefore imaged closer to the shower direction in the camera plane. A typical emission angle for DC-light is 0.15° to 0.3°, whereas most of the EAS-light is emitted at angles greater 0.4° from the direction of the primary particle. The H.E.S.S. Cherenkov cameras,

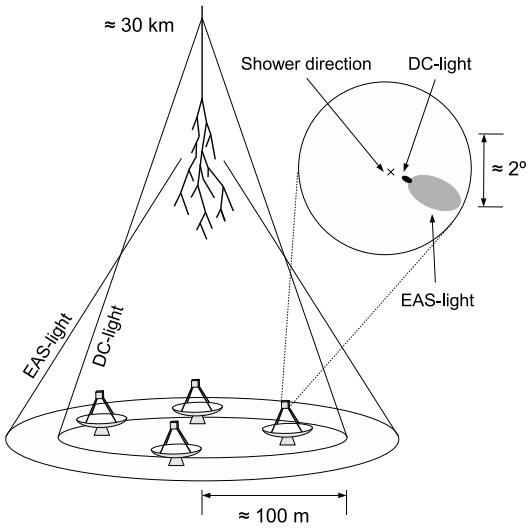

Figure 1: Schematic representation of the Cherenkov emission from a cosmic-ray primary particle and the light distribution on the ground and in the camera plane of an IACT.

with pixel sizes of 0.16°, are therefore able to resolve the DC-emission as a single bright pixel between the reconstructed shower direction and the *center of gravity* (cog) of the EAS-image in the camera plane (Fig. 1).

The energy range over which this technique can be applied depends on the charge of the primary particle [2]. At lower energies the limiting factor is that the primary particle momentum must exceed the Cherenkov threshold. At very high energies, the EAS-light outshines the DC-light, making the detection of the latter impossible. The reason for this is that the intensity of the EAS-light increases approximately linearly with energy, whereas the amount of emitted DC-photons remains basically constant above a certain energy. Because of their large atomic number and high flux compared to other heavy elements, iron nuclei are well suited for DC-light detection. The lower energy threshold for the detection of these nuclei is ~ 10 TeV.

H.E.S.S. Data

A total of 357 hours live time of H.E.S.S. data were considered for the analysis. The camera images were calibrated and the particle energy and direction were reconstructed using the standard H.E.S.S. analysis [3, 4]. Afterwards, the DC-Light is identified as a single high intensity pixel in the aforementioned angular area of the camera (Fig. 1). Once a DC-light pixel is found in a camera image, the DC-light intensity $I_{\rm DC}$ is reconstructed by subtracting the mean intensity of the neighboring pixels $I_{\rm neighb.pixels}$ from the DC-pixel intensity:

$$I_{\rm DC} = I_{\rm DC-pixel} - < I_{\rm neighb.pixels} > \quad (1)$$

In total 1899 events with DC-light detection in at least two camera images were found in the data-set (events with DC-light detection in only one camera image were not considered in the analysis to minimize systematic uncertainties [5]). The elemental composition of these events is estimated using the Z dependence of the DC-light intensity. The reconstructed charge Z^* is defined as:

$$Z^* = d(E,\theta)\sqrt{I_{\rm DC}}, \quad (2)$$

where θ is the zenith angle, E the reconstructed energy of the particle and $d(E,\theta)$ is a factor that normalizes the mean of the Z^* distribution from iron simulations to the atomic number Z of iron. The fraction $k_{\rm Fe}$ of iron events among the data is then measured by a two-component model fit to the Z^* distribution of the data. The first component of this model is the Z^* distribution of simulated iron nuclei. The second component is a sum of the Z^* distribution of lighter nuclei. The relative composition of the lighter charge bands (= all except the iron band, defined as Z>24) is kept fixed to a reference composition, so that $k_{\rm Fe}$ is the single free parameter of the fit. The reference composition is taken from the elemental flux compilations given in [11, 1]. The flux errors of these compilations are afterwards propagated into the fit result.

Iron Flux

The iron fraction in the data was measured in five energy bins. The differential iron flux $\phi(E)$ can then be estimated in each bin as:

$$\phi(E) = \frac{N_{\rm DC}(E)}{A_{\rm eff}(E)\cdot\Delta E\cdot t}\cdot k_{\rm Fe}, \quad (3)$$

where $N_{\rm DC}(E)$ is the number of detected DC-events in the energy interval from E to $E+\Delta E$,

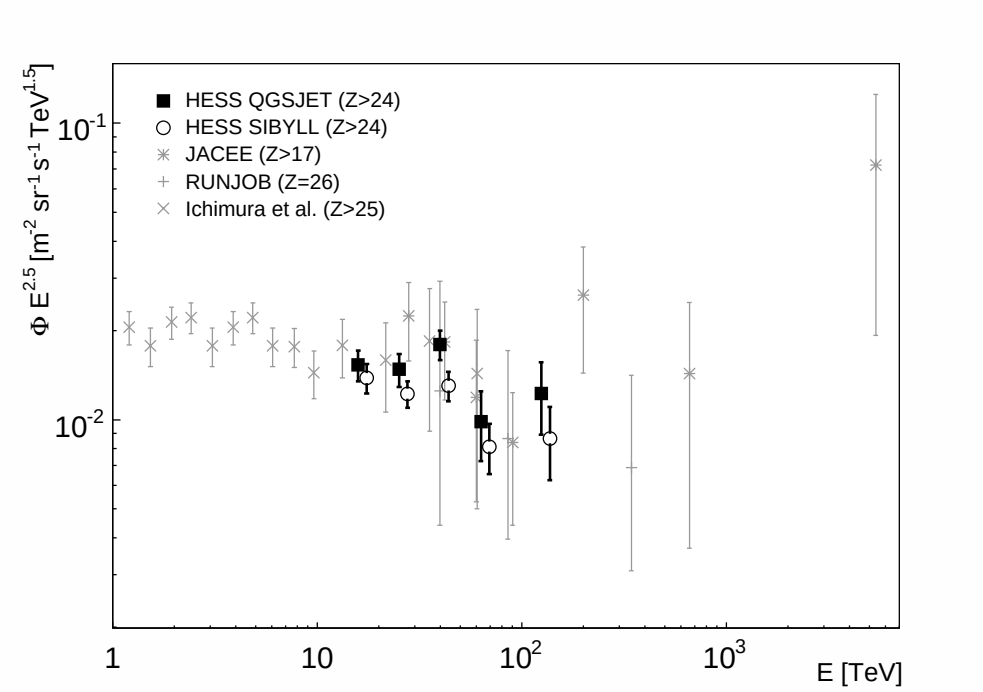

Figure 2: Differential iron energy spectrum measured with H.E.S.S. for the hadronic models QGSJET and SIBYLL multiplied by $E^{2.5}$ for better visibility of structures. The spectral points for both models are measured for the same energies. For better visibility the SIBYLL points were shifted 10% upwards in energy. The error bars show the statistical errors. The systematic flux error in each bin is 20%. The measurements from balloon experiments with data points at the highest energies are shown for comparison [8, 10, 9]. When comparing the measurements one should bear in mind that the experiments have different charge thresholds for their definition of the iron band (see legend).

t is the total live-time of the data-set and $A_{\rm eff}$ is the mean effective area times the field of view of the detector, averaged over the zenith angle of the observations, taking into account the efficiency of selection cuts.

$A_{\rm eff}$ is derived from atmospheric shower simulations of iron nuclei. These simulations rely on the detailed modeling of the hadronic interaction in EAS-showers at energies that are not accessible to current particle accelerators. To assess the systematic errors arising from uncertainties in these interactions, the analysis is performed with simulations based on two independent hadronic interaction models, SIBYLL 2.1 [13] and QGSJET 01f [12].

The resulting iron energy spectrum is shown in Fig. 2 for both hadronic models, together with the highest energy baloon measurements. The derived spectra agree well with these measurements for both models and are well fit by a power law $\phi(E) = \phi_0(\frac{E}{\rm TeV})^{-\gamma}$. The best fit values for the SIBYLL spectrum are given by $\phi_0 = (0.029 \pm 0.011)$ m^{-2}sr^{-1} TeV^{-1} and $\gamma = 2.76 \pm 0.11$ with an χ^2/ndf of 3.0/3. For the QGSJET spectrum the best fit values are $\phi_0 = (0.022 \pm 0.009)$ m^{-2}sr^{-1} TeV^{-1} and $\gamma = 2.62 \pm 0.11$ with χ^2/ndf of 5.3/3.

The difference between the two measured spectra gives an estimate of the systematic error introduced due to hadronic modeling. We note that, despite this uncertainty, the presented measurement is the most precise so far in its energy range. The result confirms the flux measurements from balloon ex-

periments with an independent technique, giving confidence in both results.

Outlook

Future improvements of the DC-light technique could extend the energy range of the measurement to an energy of $\sim$ 1 PeV. Besides larger statistics, this extension requires additional separation power of the DC-light from the EAS-light. As shown in [2], additional separation power can be achieved using the time structure of the DC-light, since it arrives with a typical delay of 4 ns with respect to the EAS light. This fact could not be exploited in the analysis presented because the H.E.S.S. data used here were taken with the standard integration window of 16 ns. However, current and planned Cherenkov telescopes, which routinely store pulse timing information [6, 7], may take advantage of this characteristic.

Due to the strong dependence of the DC-light yield on the charge of the primary particle, the DC-light technique has great potential for composition measurements. The limiting factor in the charge resolution is currently the accuracy of shower reconstruction. However, future IACT's, with pixels of smaller angular size and more nearby telescopes could provide the needed reconstruction accuracy [5].

Acknowledgements

The support of the Namibian authorities and of the University of Namibia in facilitating the construction and operation of H.E.S.S. is gratefully acknowledged, as is the support by the German Ministry for Education and Research (BMBF), the Max Planck Society, the French Ministry for Research, the CNRS-IN2P3 and the Astroparticle Interdisciplinary Programme of the CNRS, the U.K. Science and Technology Facilities Council (STFC), the IPNP of the Charles University, the Polish Ministry of Science and Higher Education, the South African Department of Science and Technology and National Research Foundation, and by the University of Namibia. We appreciate the excellent work of the technical support staff in Berlin, Durham, Hamburg, Heidelberg, Palaiseau, Paris, Saclay, and in Namibia in the construction and operation of the equipment.

References

[1] H. Meyer B. Wiebel-Sooth, P. L. Biermann. Individual element spectra: prediction and data. *Astronomy & Astrophysics*, 330:389, 1998.

[2] S.P. Swordy D. B. Kieda and S.P. Wakely. A high resolution method for measuring cosmic ray composition beyond 10 TeV. *Astroparticle Physics*, 15:287, 2001.

[3] F. Aharonian et al. Calibration of cameras of the H.E.S.S. detector. *Astroparticle Physics*, 22:109, 2004.

[4] F. Aharonian et al. Observations of the Crab Nebula with H.E.S.S. *Astronomy & Astrophysics*, 457:899, 2006.

[5] F. Aharonian et al. First ground based measurement of atmospheric Cherenkov light from cosmic rays. *Phys. Rev. D*, 75:042004, 2007.

[6] J. Cortina et al. Technical Performance of the MAGIC Telescope. *Proc. 29th ICRC, Pune*, 5:359, 2005.

[7] J. Holder et al. The first VERITAS telescope. *Astroparticle Physics*, 25:391, 2006.

[8] K. Asakimori et al. Energy Spectra and Elemental Composition of Nuclei above 100 TeV from a Series of the JACEE Balloon Flight. *Proc. 24th ICRC, Rome*, 2:707, 1995.

[9] M. Ichimura et al. Observation of heavy cosmic-ray primaries over the wide energy range from $\sim$100 GeV / paticle to $\sim$100 TeV / particle: Is the celebrated knee actually so prominent? *Phys. Rev. D*, 48:1949, 1993.

[10] V. A. Derbina et al. Cosmic-ray spectra and composition in the energy range of 10-100 TeV per particle obtained by the RUNJOB experiment. *The Astrophysical Journal*, 628:L41, 2005.

[11] J. R. Hörandel. On the knee in the energy spectrum of cosmic rays. *Astroparticle Physics*, 19:193, 2003.

[12] A. I. Pavlov N. N. Kalmykov, S. S. Ostapchenko. Quark-gluon-string model and EAS simulation problems at ultra-high energies. *Nucl. Phys. B (Proc. Suppl.)*, 52, 1997.

[13] P. Lipari T. Stanev R. S. Fletcher, T. K. Gaisser. SIBYLL: An event generator for simulation of high energy cosmic ray cascades. *Phys. Rev. D*, 50:5710, 1994.